Natkhin *et al. Annals of Forest Science* (2026) 83:5
https://doi.org/10.1186/s13595-025-01318-2

INRAE

Annals of Forest Science

RESEARCH

Open Access

Impact of extreme precipitation events on summer deep seepage below temperate forests in the Northeastern Germany lowlands

Marco Natkhin[1*], Maximilian Strer[1], Tanja GM Sanders[1], Tobias Schad[1] and Kai Schwärzel[1]

Abstract

Key Message Stands stocked with European beech (*Fagus sylvatica* L.), sessile oak (*Quercus petraea* (Matt.) Liebl.), and Scots pine (*Pinus sylvestris* L.) show distinct deep seepage patterns. An increasing importance of extreme summer precipitation contributing to deep seepage in the northeastern German lowlands was detected. Extreme summer precipitation events contributed 71% (pine), 22% (young oak), and 15% (beech) of the annual deep seepage. Adapted forest management may promote deep seepage caused by extreme summer precipitation and by precipitation during the winter half-year.

Context To date, deep seepage and groundwater recharge in temperate lowland forests occured mainly during the winter half year, the only period in which precipitation exceeds potential evapotranspiration. The increasing occurrence of extreme summer precipitation events, however, has the potential to promote deep seepage during summer.

Aims This study aims to quantify the deep seepage feed by extreme summer precipitation events, utilising three large-scale lysimeters below canopies of beech (*Fagus sylvatica* L.), young oak (*Quercus petraea* (Matt.) Liebl.), and pine (*Pinus sylvestris* L.), respectively.

Methods Using a seepage hydrograph separation method, we were able to identify two major types of deep seepage: slow deep seepage due to winter precipitation and rapid deep seepage due to extreme summer precipitation events.

Results Our measurements attributed substantial portions of deep seepage to extreme summer precipitation events, with distinct differences among lysimeters related to tree species and stand structure. The highest ratio of deep seepage by extreme summer precipitation to annual deep seepage occurred below pine, whereas the highest quantities of deep seepage by extreme summer precipitation were found under young oak.

Conclusion Rapid deep seepage due to an increase in extreme summer precipitation events could be the most important mechanism for recharging near-surface groundwater aquifers under pine forests in the northeastern Germany lowlands. Deep seepage may be influenced by the choice of tree species and stand structure.

Keywords Deep seepage , Forest hydrology, Large-scale lysimeter, Northeastern Germany lowlands, Intensive forest monitoring station Britz

Handling editor: Erwin Dreyer

*Correspondence:
Marco Natkhin
marco.natkhin@thuenen.de
Full list of author information is available at the end of the article

1 Introduction

The dryingup of northeastern German lowland aquifers in recent decades affecteds lakes and streams in various ways (Kaiser et al. 2014; Lischeid et al. 2021). The predicted increase in summer dry periods, rising temperatures, and shifting rainfall patterns will likely exacerbate the negative trend in groundwater levels and their potential for recharge (Wunsch et al. 2022). In this region, the low groundwater recharge is linked to the dry climate in combination with the extensive pine (*Pinus sylvestris* L.) forests, which allow little or no deep seepage (Müller and Bolte 2009; Leuschner et al. 2022). However, altering weather patterns leading to extreme summer precipitation events (Kreienkamp et al. 2021; Hänsel et al. 2022; Ibebuchi 2022) might have a noticeable impact on the recent and prospective water balance.

In general, the mean long-term groundwater recharge is fed by precipitation and lowered by several factors (e.g., interception) (Scanlon et al. 2002). Only water leaving the rooting zone, no longer accessible for plants, is classified as deep seepage, which can then recharge groundwater aquifers. In the northeastern German lowlands, evapotranspiration normally exceeds the amount of precipitation during the growing season, whereas limited solar irradiance limits plant growth, root water uptake, and evapotranspiration during the winter months. Over the course of the year, evergreen pine stands show larger evapotranspiration than beech (*Fagus sylvatica* L.) or oak (*Quercus petraea* (Matt.) Liebl.) (Müller and Bolte 2009). Young trees with less developed roots and canopies transpire less than mature trees (Haydon et al. 1997; Oishi et al. 2020). In temperate regions, soil water withdrawn by plant roots during the growing season is gradually replenished by autumn and winter precipitation. Therefore, in our study region, seepage usually occurs during the winter months as soon as soil water content exceeds field capacity (Schwaiger et al. 2018).

Over the last two decades, shifting precipitation patterns occurred, including increases in climate extremes, e.g., drought or heavy precipitation events (Metzger et al. 2008; Djebou et al. 2016; Hosseinzadehtalaei et al. 2020). Rakovec et al. (2022) concluded that the multiyear drought of 2018–2020 not only set a new benchmark but also gave a sneak preview into the future. This exceptionally dry period led to large summer water deficits which were not compensated by the subsequent winter precipitation, as quantifications with the GRACE Follow-On satellite mission showed (Boergens et al. 2020). However, this exceptional drought came with some remarkable extreme summer precipitation events, especially in the northeastern German lowlands (Deutscher Wetterdienst 2018, 2019, 2020; Kreienkamp et al. 2021; Ibebuchi 2022). The influence of this cascade of extreme meteorological events on the hydrological processes has hardly been investigated yet, since they often occurred locally and with a high spatial heterogeneity (Miegel et al. 2014).

In catchment hydrology, the effects of heavy precipitation on river discharge are commonly analysed via the hydrograph separation method, i.e. separation of slow base flows and fast direct runoffs (e.g. Lei-lei et al., 2011; Kissel and Schmalz 2020). Discharge measurements with daily or, even better, hourly resolution are essential for separating these fast direct- and slow base-flow components (Wittenberg et al. 2019). During heavy rainfall, the infiltration of water into the soil results in a rapid increase in soil moisture, first in the topsoil and then in the subsoil (e.g., Schwärzel et al. 2009). Such events can ultimately lead to deep seepage, which can be detected by discharge measurements in lysimeters (Meißner et al. 2010). The use of lysimeters offers the only direct measurement of deep seepage (Scanlon et al. 2002; Müller and Bolte 2009; Gong et al. 2021). Seepage hydrograph separation allows for allocation of fractions of seepage to specific events during deep seepage.

From 2018 to 2021, every summer, a heavy precipitation event with more than 60 mm rainfall within 24 h occurred. This study aims to analyse the impacts of these four heavy summer precipitation events from 2018 to 2021 on deep seepage formation under different species (European beech (*Fagus sylvatica* L.), sessile oak (*Quercus petraea* (Matt.) Liebl.), and Scots pine (*Pinus sylvestris* L.). For this purpose, we analysed the daily deep seepage along with other parameters monitored by the intensive forest monitoring station Britz, Germany, via the seepage hydrograph separation method and large-scale lysimeters. The specific objectives of this study were as follows: (1) To examine whether the observed abundance of extreme summer precipitation events was increasing, (2) to identify and quantify the impact of extreme summer precipitation events on deep seepage by applying the seepage hydrograph separation method to the site monitoring data, and (3) to analyse whether the influence of tree species and stand structure on the water balance was also evident under extreme summer precipitation events.

2 Material and methods

2.1 Site description

The intensive forest monitoring site "Britz" (hereafter IFMS Britz) in Brandenburg, Germany (52°52′41″ N 13°50′2″ O), is operated by the Johann Heinrich von Thünen Institute—Institute of Forest Ecosystems (Krause et al. 2019; Sanders and Natkhin Sanders 2025). Regular measurements started in the early 1970s to quantify the effects of different tree species on groundwater recharge in the northeastern German lowlands under identical

soil and climatic conditions. The climate is transitional between marine and continental humid winters (Cfb (Kottek et al. 2006), Dfb (Beck et al. 2018)). The annual mean precipitation sum is 618 mm, and the annual mean temperature is 9.0 °C (1991–2020). The precipitation regime is dominated by two main events: mostly short-lived and isolated thunderstorms/storm cells versus west-wind bound frontal systems originating from the Atlantic Ocean. While the latter occurs throughout the year and leads to a substantial amount of precipitation, isolated heavy thunderstorms can provide notable amounts of precipitation during single, short-term events. These events typically occur in the hydrological summer half-year (here May to October) between June and August. The soil at the site, derived from Pleistocene sand deposits (Don et al. 2019), is a dystric cambisol with a medium sand texture (Table 1).

The site is divided into subplots, each measuring approximately 60 by 40 m, stocked with either European beech (*Fagus sylvatica* L.), sessile oak (*Quercus petraea* (Matt.) Liebl.), or Scots pine (*Pinus sylvestris* L.) in pure stands. Beech and pine stands were planted in 1974, and the oak stands in 1999, hereafter oak (y), to emphasise the differences in stand age (Table 2). All three species represent the typical forest vegetation of the area, with pine dominating and beech and oak representing the potential vegetation. A large-scale lysimeter is located at the centre of each of the three analysed subplots. Differences in measured water balance are attributed to differences in stands, with no replication.

2.2 Measurements

The large-scale lysimeters with an area of 100 m^2 each (Müller and Bolte 2009) collected deep seepage water at a depth of approximately 5 m, with the groundwater table being located approximately 15.6 m beneath ground level (July 2023). For each stand, we analysed the lysimeters' outflow with a registering tipping gauge (PC by Umwelt-Geräte-Technik GmbH) providing seepage water time series at a resolution of 1/1000 mm (0.1 L per tip). The soil in the lysimeters was disturbed due to the building of the lysimeters. However, it was reconstructed to resemble the soil profile previously found on site (Table 1) and remained undisturbed since installation. The site is flat, and the infiltration of sand is high; therefore, no surface runoff occurred.

Table 2 Stand properties measured in 2023. Leaf area index was measured with an optical device, Solariscope SOL300, without ground vegetation in July 2023. Tree height was measured with a Vertex V (Haglöf, Sweden AB), and the diameter at breast height was measured with a calliper

	Beech	Oak (y)	Pine
Planted (year)	1974	1999	1974
Tree density (trees/ha)	1040	3360	1090
Mean diameter at breast height (cm)	15.1	5.4	20
Mean tree height (m)	17	6.5	19.8
Leaf area index (m^2/m^2)	4.4	2.4	1.5

Precipitation was recorded by a tipping bucket with a magnetic reed switch (by LAMBRECHT meteo GmbH; type: 15,189, orifice area: 200 cm^2, resolution: 0.1 mm, temporal aggregation to 15 min, accuracy: ±2%, 0.8 mm/min load). The device was installed 1 m above ground level in the open field according to Raspe et al. (2020). On the basis of these measurements, we were able to derive a consistent time series of daily precipitation for the four analysed events and for long-term precipitation trend analysis from 1 st January 1993 to 31 st December 2022 for the site, supplementing minor gaps via linear regression via local parallel measurements. For this purpose, two other automatic gauges at 0 and 1 m above ground and two manually read-out gauges were available. The insufficient data before 1993 limits the time series. Systematic precipitation measurement errors were corrected after Richter (1995).

To estimate the interception losses, monthly manual gauges were read out under the canopy, with 12 at each

Table 1 Parameters of mineral soil horizons at the IFMS Britz, Germany: horizon symbols according to IUSS Working Group WRB (2022) and grain size distribution according to A. G. Boden et al. (1994) with sand: 0.63–2 mm, clay < 0.002 mm, and silt: between 0.002 and 0.063 mm

Horizon	Thickness (cm)	Soil texture class	Bulk density (g cm^{-3})	Fraction (%)		
				Sand	Clay	Silt
Eh	1	S				
Bhg	15	S	1.19	94	2	4
Bg-C	10	S	1.5	98	0	2
C	66	S	1.59	99	0	1
ρGo-C	> 100	S	1.66	97	0	3

forested stand and 6 at the open field site, according to the ICP Forests Manual (Raspe et al. 2020).

In this study, the amount of precipitation observed during extreme summer precipitation events corresponds to the amount of precipitation recorded within 24 h. Precipitation events occurring prior to and after the events under analysis were also taken into account in our analysis as "extended" precipitation, as they may also provide a substantial amount of water to deep seepage formation. To consider these effects, Sobaga et al. (2024) used an extended precipitation period of 10 days. Our lysimeters are larger and deeper, and hence, it takes longer for the infiltrating water to reach the lysimeter base; we therefore used twice the time and added up the precipitation over a maximum period of 20 days. This approach was not used to quantify water fluxes but rather to set the precipitation more appropriately in relation to related deep seepage.

The soil water content was measured at 10 depths to 4.6 m with three sensor tubes on every plot with a capacitive Sentek EnviroSCAN tube. The measurements started with the installation of these sensors during 2010. The data used in this paper is accessible at Natkhin et al. (2025).

2.3 Calculations

2.3.1 Long-term water balance

The mass balance equation was used to compute the long-term water balance and establish a baseline for our analysis of the impact of tree species and age structure after extreme summer precipitation events. In the case of deep seepage, the annual water balance equation is as follows:

$$P = ET + Q + \Delta S \tag{1}$$

with P: annual precipitation in the open field in mm/year, ET: evapotranspiration in mm/year as the remainder in this balance, Q: measured mean annual sum of deep seepage in mm/year, and ΔS: mean annual change in water storage S in mm/year. ΔS is defined as the difference between the end and start of the balance period divided by the number of years of the balance period. S calculates as follows:

$$S = \sum_{n=1}^{10} (\Theta_n h_n) \tag{2}$$

with n: sensor number; Θ_n: volumetric water content of the nth layer, which is measured at 10 depths (0.1–4.6 m); and h_n: layer thickness in mm, assuming that every measurement is representative of the median between the next sensor depth or the upper or lower ground of the lysimeter. A time span of 2013–2023 was used to calculate the water balance. This time span was chosen due to sufficient data availability to calculate the balance components.

The available soil water content (AWC) is a scaled water content:

$$AWC = \frac{WC - PWP}{Fc - PWP} \tag{3}$$

with Fc: field capacity and PWP: permanent wilting point. The particle size distribution was determined from soil samples analysed in our laboratory (Cools and De Vos B., 2020). Fc and PWP were estimated by a pedotransfer function with 12% and 4%, respectively (A. G. Boden et al. 1994).

2.3.2 Identification of deep seepage by extreme summer precipitation events

The flow separation is based on the time series of daily values of precipitation and measured deep seepage. The measured deep seepage q in mm/day is separated into deep seepage caused by extreme precipitation events (q_e) and deep seepage caused by precipitation during the winter half-year (q_w):

$$q = q_w + q_e \tag{4}$$

This method is adapted from the widely used baseflow separation method in catchment hydrology (Wittenberg 1999; Wittenberg and Sivapalan 1999; Eckhardt 2008; Lei-lei et al. 2011). Our approach is based on following assumptions: q_w occurs slowly along the matrix flow using small pores, such as a linear reservoir with an annual maximum and an exponential decrease afterwards, showing a clear declining trend (Fig. 1, black line). In contrast, q_e (Fig. 1, green line) occurs after an extreme event, through a fast matrix flow via larger pores and pathways, e.g. root canals quickly reach a local peak after the measured precipitation event. Figure 1 illustrates the time lag between the peaks of q_w and q_e, enabling a clear separation between the two types of seepage.

To identify deep seepage caused by extreme summer precipitation events (q_e), the day of a defined extreme precipitation event (t_p) is set as the starting point for the search algorithm. The date of the first local minimum of d after t_p is assumed to be the starting point t_c for the extreme event that feeds q_e. However, there are two possible cases of flow separation. If deep seepage is 0 mm/day at t_c, then it can be assumed that deep seepage (q_w) caused by winter precipitation has already ceased. Therefore, the new seepage occurring at this time is completely attributed to q_e. However, if $q(t_c) > 0$ mm/day, then q_e must be separated from q_w.

We developed a procedure based on fitting an exponential function to model the decrease in deep seepage in winter. During the occurrence of a deep seepage event

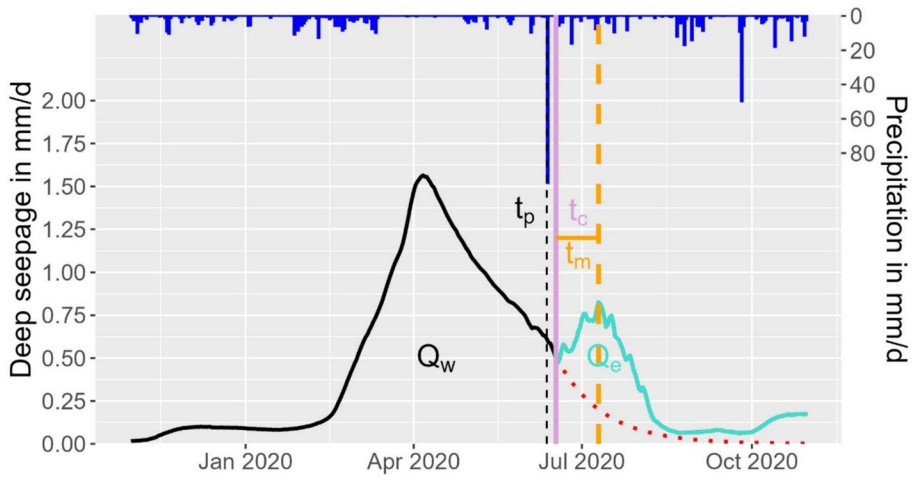

Fig. 1 Schematic deep seepage hydrograph with flow separation. q_w, winter precipitation fed seepage; q_e, extreme event fed deep seepage; t_p, time of precipitation event; t_c, response time until event's impact on deep seepage curve; t_m, time span from the start to the peak of q_e; dotted line, separation between q_w and q_e

q_e, the winter seepage q_w is determined by the function $R(t)$, which describes the exponential decrease in q_w after its maximum. The function parameters R_0 and K are fitted to q_w before the deep seepage event. We use the *nls* function of the *stats* package in R (version 4.2.2) to fit this function (R Core Team 2022). Afterwards, $R(t)$ is extrapolated for $t > t_c$ and subtracted from the total deep seepage time series after its local minimum. This separates the fading winter deep seepage from the event-specific deep seepage. $R(t)$ is defined as follows:

$$R(t) = R_0 \cdot e^{-\frac{t}{K}} with R(t_c) = R_0 \tag{5}$$

where t is the time in days, K is an exponential parameter, and R_0 is the intercept of the function. The duration between an extreme precipitation event and when q_e reaches its maximum is t_m. The daily deep seepage fluxes are summed from the 1st November of the previous year to the 31st of October of the year when the extreme event occurred (hydrological year (DIN 4049, 1992)) to the annual deep seepage sums in millimetre:

$$Q_e = \sum q_e \tag{6}$$

$$Q_w = \sum q_w \tag{7}$$

$$Q_{sum} = Q_w + Q_e \tag{8}$$

2.3.3 Return periods of extreme precipitation

Extreme summer precipitation events are rare; their return period is of high interest. The analysis of precipitation measurements at the IFMS Britz revealed that heavy precipitation events usually occurred during the meteorological summer (JJA — June, July, August). To estimate the return period of extreme summer precipitation events, we conducted a stationary extreme value analysis. We first calculated the block maxima for the JJA period. The block maximum in our case is the maximum daily precipitation amount within JJA:

$$X_{ext}\prime(i) = max(\{X(i)\}|T(i) \tag{9}$$

where $X_{ext}\prime(i)$ represents the block maxima per meteorological summer, $X(i)$ represents the JJA time series, and $T(i)$ represents the ith year of the time series. We used the block maxima to fit a generalised extreme value distribution and to conduct a trend analysis of the return periods. This method is used for extreme precipitation analysis (e.g. Lazoglou et al. 2019; Courty et al. 2019; Passow and Donner 2019). We examined the abundance and shifts in extreme summer precipitation with a more pragmatic pseudo-nonstationary approach. Instead of calculating time-dependent parameters for each parameter of the distribution, we recalculated the parameter within a moving window of 20 years and the return period for the different windows.

To identify shifts in precipitation patterns, we calculated the event duration (consecutive days with precipitation amounts > 1 mm per day) and the proportion of total summer precipitation for each single event.

3 Results

3.1 Extreme precipitation events

We identified four extreme summer precipitation events in the following months: July 2018, June 2019, June 2020, and June 2021 (Table 3). Those four

Table 3 Characteristics of the four extreme summer precipitation events: event dates, beginning of precipitation, duration, statistical return periods from 1993 to 2022, and the extended precipitation includes adjacent precipitation events

Event ID	Event date	Precipitation amount† (mm)	Event duration (hour)	Return period (year)	Extended precipitation† (mm)	Extended duration (days)
Event18	2018 July 09	80	18	41	115	4
Event19	2019 June 05	67	9	28	131	13
Event20	2020 June 13	82	9	45	112	14
Event21	2021 June 30	150	24	200	174	17

†Precipitation corrected after Richter (1995)

events ranked at the top of the extreme events in terms of the amount of precipitation. We devised the following nomenclature to address extreme events and lysimeters: we combined the tree species of the lysimeter and occurrence year (EventYY) of a precipitation event with (e.g. Pine18–pine lysimeter measurement–extreme event of 2018). The identified extreme summer precipitation events reached (Event19) or even exceeded (Event21) the monthly mean of precipitation (67.5 mm) over the period 1993–2022. These events lasted up to 24 h. The days with exceptionally high precipitation are embedded in extended periods (maximum 20 days) of precipitation (Table 3), potentially enhancing the effects of the short extreme events related to deep water seepage.

The statistical return periods with spans of 28–200 years emphasise the extreme nature of the recorded precipitation events (Table 3). We found a general downwards trend for precipitation levels above 50 mm per day (Fig. 2): While 80 mm of daily precipitation had a return period of 90 years at the beginning of our analysis period, it decreased to 30 years at the end. Starting with a return period of approximately 300 years, even a daily precipitation amount of 120 mm reaches a return period of 70 years at the end of our analysis period. Regarding the first special objective, this indicates high-precipitation events became more frequent over the observed period.

No trend was identified in the total summer precipitation (1993–2022) (Mann–Kendall test). We found no

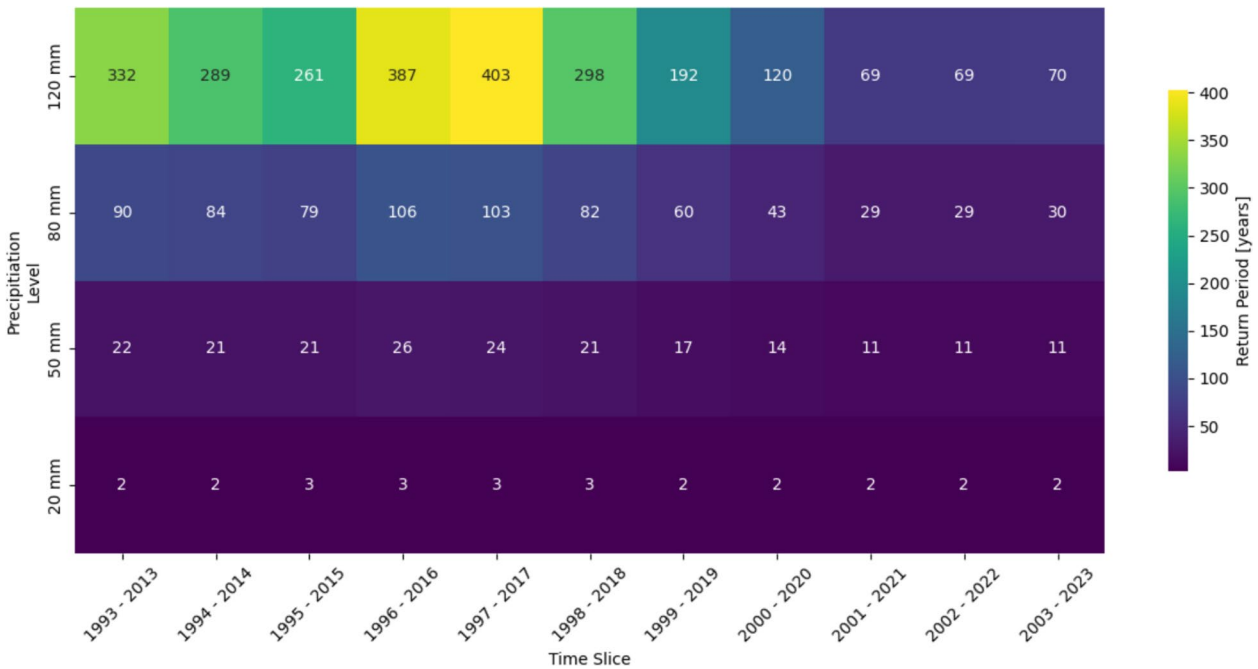

Fig. 2 Heat map of return periods for selected daily precipitation levels of 20, 50, 80, and 120 mm, segmented into consecutive 20-year periods. The colours indicate the magnitude of the return periods

clear trend regarding event duration. However, we found a significant increasing trend in the maximum single event per summer and its contribution to total summer precipitation ($p=0.05$). The contribution of extreme summer precipitation events to total summer precipitation was between one-quarter in 2020 and almost half in 2021 (Table 4).

3.2 Impact of extreme summer precipitation events on deep seepage

Extreme summer precipitation events occurred, while Q_w decreased or ceased but did not increase. A visual inspection (Fig. 3) revealed that the occurrence of deep seepage was a result of heavy precipitation given the additional seepage peaks in the graph, which occurred after the Q_w maximum. These peaks were characterised by sharper and steeper gradients than those resulting from winter precipitation.

Rapid deep seepage induced by extreme precipitation was observed in the lysimeter with oak (y) during 2018, 2019, 2020, and 2021, with beech in 2020 and 2021, and with pine in 2018 and 2021 (Fig. 3, Table 4). Event21 presented the highest precipitation amount and led to the highest Q_e for all stands, whereas the event in 2018 produced the lowest Q_e.

According to the second special objective, Table 5 lists characteristic values for classifying and assessing deep seepage events triggered by extreme summer precipitation events (Table 4). The onset of deep seepage varied by event and tree species, but the number of events was too small to identify patterns. The maximum degree of heavy precipitation-induced deep seepage was reached after 6–27 days.

3.3 Water balance of the different stands

3.3.1 Components of long-term water balance

The mean annual values of the water balance components for beech, oak (y), and pine are presented in Table 6. From 72% (young oak) up to 97% (pine) of the annual precipitation was used by evapotranspiration. Annual deep seepage in the lysimeter below pine remained very low, whereas under beech, approximately 10% of the annual precipitation contributed to deep seepage. In the lysimeter with young oaks, approximately one-third of the average annual precipitation contributed to deep seepage.

Table 4 Precipitations during years with extreme summer precipitation events

Year	P_e (mm)	P_W (mm)	P_{summer} (mm)	P_e/P_{summer} (%)
2018	115	309	275	42
2019	131	215	416	31
2020	112	233	407	28
2021	174	221	370	47

P_w, precipitation of the winter half-year (November–April); P_e, extended precipitation of extreme events (see Table 3); P_{Summer}, total summer precipitation including extended precipitation of extreme events (May–October)

3.3.2 Deep seepage caused by winter precipitation

Figure 3 revealed that the dynamics of deep seepage formation (Q_w) triggered by winter precipitation differs for the three lysimeters. We observed no or only a small amount of deep seepage below pine. Also, soil below pine is drier throughout the years (Fig. 4).

In contrast to pine, the amount of deep seepage linked to precipitation during the winter half-year (Q_w) was generally much larger below beech and oak (y). Yet, in 2019, for the first time since measurements began, no deep seepage was observed under beech. Moreover, the maximum amount of soil water stored in the soil profile under beech was lower during 2019 than during the other 3 years with extreme summer precipitation events (Fig. 4). The infiltration values of Q_w were larger under oak (y) than under beech and pine (Table 4). Deep seepage formation due to winter precipitation (Q_w) generally lasted longer under oak (y) than under beech. In addition, the peak values of deep seepage (Fig. 3) and the maximum soil water storage (Fig. 4) were larger below oak (y) than beech every year.

The curve of daily deep seepage values (Q_w) in 2018 for beech and oak (y) shows two distinct maxima. One maximum of daily deep seepage occurs in winter (mid-February), and the other is reached in spring (early May). Both maxima were fed by winter precipitation in the winter of 2017/2018. From April 2018 onwards, the seepage rates increased again and reached their maximum in May 2018.

3.3.3 Stand-specific deep seepage caused by extreme summer precipitation

Regarding the third special objective, differences in soil water content (Fig. 4) can also be found before extreme summer precipitation events start, with the highest amounts occurring under young oak stands and the lowest occurring under pine stands (Table 5).

Under oak (y), we always registered the highest Q_e events in absolute values over the 4 years, with an accumulated sum of 163 mm for Q_e. This also means that Q_e accounts for 22% of the entire deep seepage for oak (y) (Fig. 5). Compared with oak (y), the absolute deep seepage rates for beech triggered by extreme summer precipitation events were lower. Nevertheless, Q_e accounts for 15% of the total deep seepage under beech. In contrast, the vast majority of the annual seepage in pine stands originate from extreme summer events, with a share of 71% (Fig. 5).

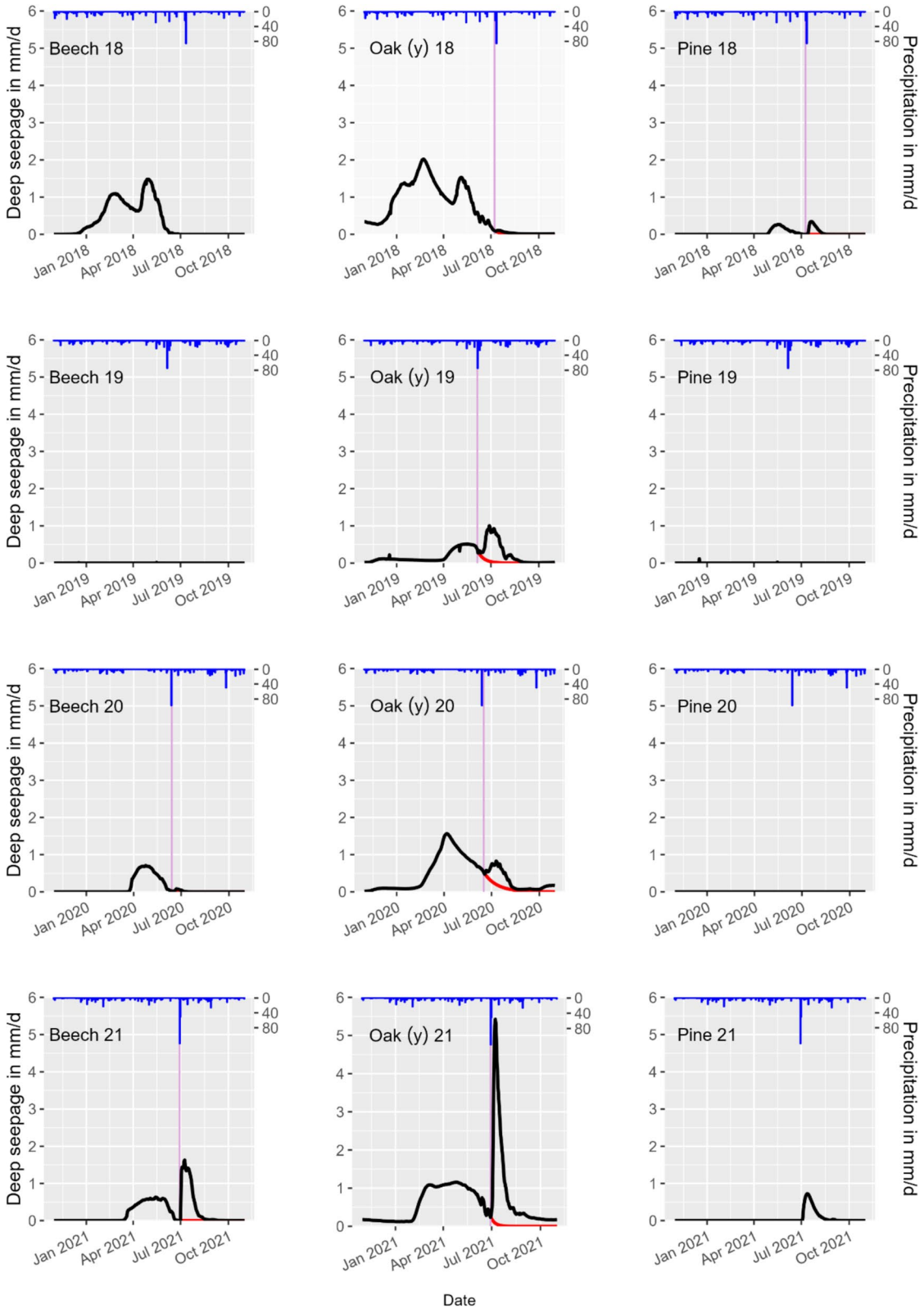

Fig. 3 Precipitation (blue bars) and deep seepage during the selected years (2018, 2019, 2020, and 2021) in the three lysimeters with three different tree species (beech (50 years), oak (20 years), and pine (50 years)). The red lines denote the separation of Q_w and Q_e

Table 5 Deep seepage (see also Fig. 3) in years with extreme summer precipitation events

Year	Stand	Q_w (mm)	Q_e (mm)	Q_{sum} (mm/year)	Q_e/Q_{sum} (%)	t_c (day)	t_m (day)	AWC_b (%)
2018	Beech	122	0	122	-	-	-	20
	Oak (y)	243	3	245	1	1	6	27
	Pine	8	6	14	39	1	11	16
2019	Beech	0	0	0	-	-	-	35
	Oak (y)	43	32	75	43	1	23	72
	Pine	0	0	0	-	-	-	21
2020	Beech	36	1	37	3	2	9	32
	Oak (y)	132	28	160	17	5	27	44
	Pine	0	0	0	-	-	-	6
2021	Beech	44	36	80	46	1	9	32
	Oak (y)	146	102	248	41	1	8	44
	Pine	0	16	16	100	4	12	9

Q_w, winter precipitation feed seepage; Q_e, extreme event precipitation feed seepage; Q_{sum}, sum of Q_w and Q_e; t_c, response time until event's impact on deep seepage curve; t_m, time span from t_c to the peak of q_e; AWC_b, soil water content (0–5 m) before the extreme event

Table 6 Water balance components for beech, oak (y), and pine trees from 2013 to 2023

Water balance components	Beech	Oak (y)	Pine
Mean annual precipitation† sum (mm)	655	655	655
Mean annual evapotranspiration (mm)	598	499	645
Mean annual interception loss (mm)	123	105	200
Mean annual deep seepage (mm)	53	170	4
Minimal annual deep seepage (mm)	0	75	0
Median annual deep seepage (mm)	37	168	0
Maximal annual deep seepage (mm)	121	265	16

†Open field precipitation corrected after Richter (1995). Evapotranspiration includes interception

4 Discussion

4.1 Meteorological extreme events

The four analysed precipitation events observed at IFMS Britz were extreme and statistically rare, even if they occurred during 4 consecutive years. The analysis revealed that extreme summer precipitation events have become more frequent over the observed period, and the return period of certain extreme events has decreased within recent years. Additionally, Hänsel et al. (2022) reported, depending on the applied indicator, an increase in extreme summer precipitation events in Europe in recent years, not yet including the exceptional extreme summer precipitation event of 2021 (Ibebuchi 2022).

The absolute amount of extreme precipitation events could be underestimated, as during high-intensity precipitation tipping gauges display reduced accuracy. Fortunately, the highest intensities during these events remained below 1 mm per minute, while the maximum load of the tipping bucket used here is specified with 8 mm per minute. Thus, we assume that the underestimation was slight.

In general, summers will become drier, and, overall, the variability is likely to increase (Vicente-Serrano et al. 2014; Pendergrass et al. 2017; Ionita and Nagavciuc 2021). These predictions could not be verified by the total summer precipitation time series of IFMS Britz. However, the share of summer precipitation during extreme events lasting 9 to 24 h to total summer precipitation was remarkable. Extreme events increased in intensity and frequency (Fischer and Knutti 2015; Qing et al. 2023). Although our study does not include any climate projection, it shows that extreme summer precipitation events may become more important for deep seepage in the future. Owing to the short series of measurements, a general impact on deep seepage cannot be assumed yet. Even if the increase in extreme precipitation events is quite certain in climate projections, the resulting risks, depending among other things on soil conditions, are much less certain (Tabari 2020). The nature of extreme summer precipitation events is a regional one, as there is a relation between the intensity and the regionality of extreme events; with an increase of the affected area, the statistical amount of extreme precipitation events decreases (Ludwig et al. 2023).

4.2 Application and validity of the Q_e separation method

To our knowledge, our study is the first to use the principles of the seepage hydrograph separation method for analysing deep seepage formation from recorded lysimeter measurements. This method allows a general attribution of input from overlapping precipitation events to a resulting output of the lysimeters' seepage hydrograph response. The need for a continuous decrease in

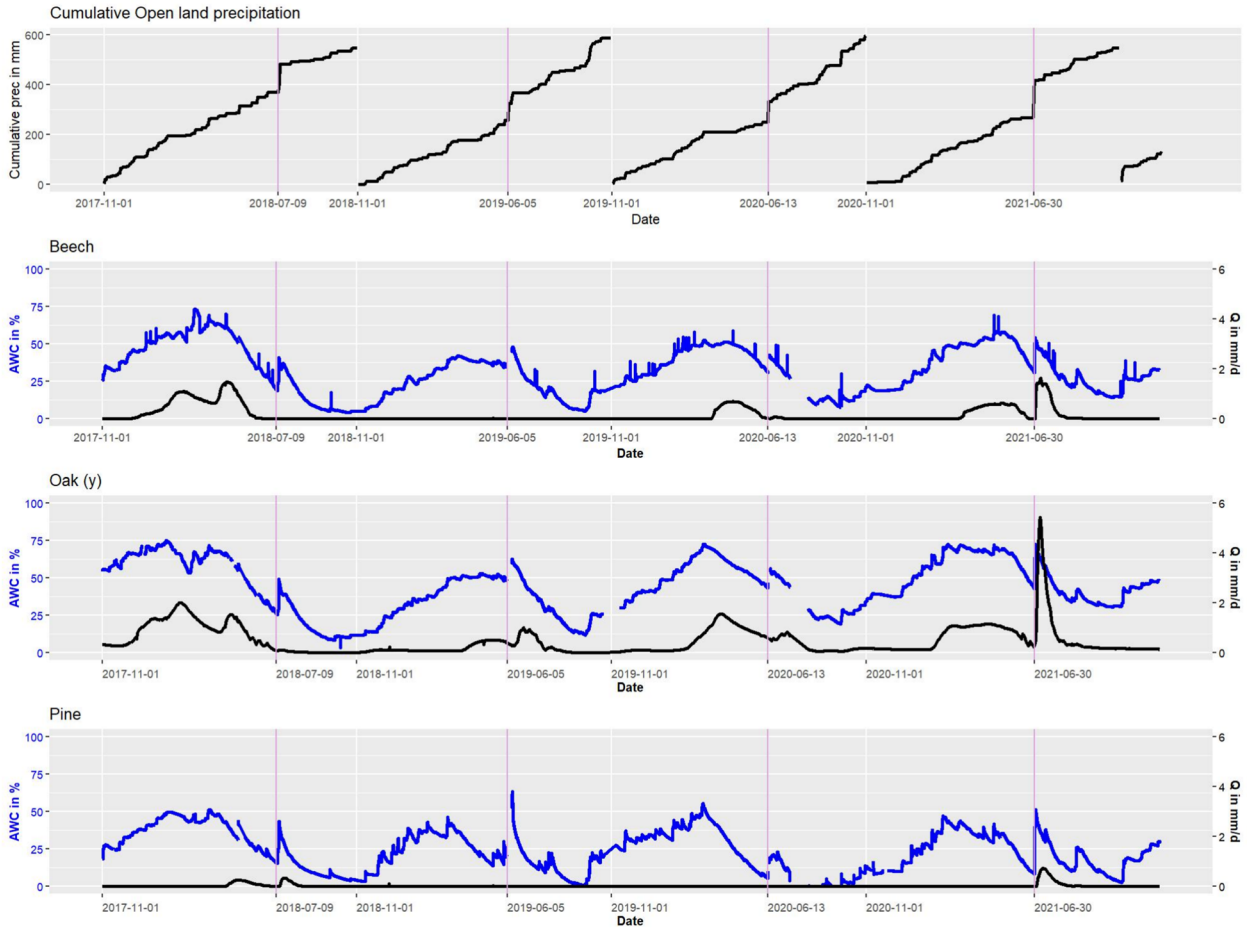

Fig. 4 Time series (2018–2021) of annual cumulative precipitation in hydrological years (November–October), available water content (AWC) in % over 5 m soil depth, and deep seepage (Q) for the three stands beech, oak (y), and pine; horizontal red lines mark the dates of the analysed extreme summer precipitation events

winterfed deep seepage Q_w over time implies, at the technical level, a distinguishable input signal that generates a clear and identifiable response in the seepage hydrograph to be separated by an exponential function. Our assumption was fulfilled through Q_e reacting quickly — the maximum peak was reached within 6–27 days after the precipitation event (compared to the slow reaction in Q_w). Wittenberg et al. (2019) reported a response time of 2 days of groundwater recharge in the northeastern German lowland. In our lysimeters, the response started within this time lapse but reached a delayed maximum, probably due to longer flow paths. In addition, there were clear time lags between the peaks of Q_w and Q_e, which makes it possible to distinguish between slow winter seepage and rapid summer seepage. The occurrence of two maxima during 2018 in the lysimeter below beech and oak(y) resulted from a winter dry spell, as only a very small amount of rain or snow fell over a period of 30 days, and no notable precipitation occurred during the period from February to March 2018. This phenomenon of two maxima before the extreme event was not observed from 2019 to 2021, as no prolonged dry spells occurred during these winters. As we focus here on the peaks caused by extreme summer precipitation events, this occurrence limits our method. The exponential decrease curves fit well (red lines in Fig. 3), indicating a linear reservoir type feeding Q_w.

Sobaga et al. (2024) analysed the impact of intense precipitation events over 45 years on agricultural soils in northeastern France via lysimeters. Their maximum precipitation event was 65.5 mm/day, which is comparable to Event19 but considerably smaller than Event21. They reported that some intense precipitation events in spring and summer caused recharge, and that accumulated precipitation above 58 mm was required for their lysimeters to generate such fluxes. While our extreme summer precipitation events constituted, on average, 35% of the annual precipitation and led to 15% (young oak) to 71%

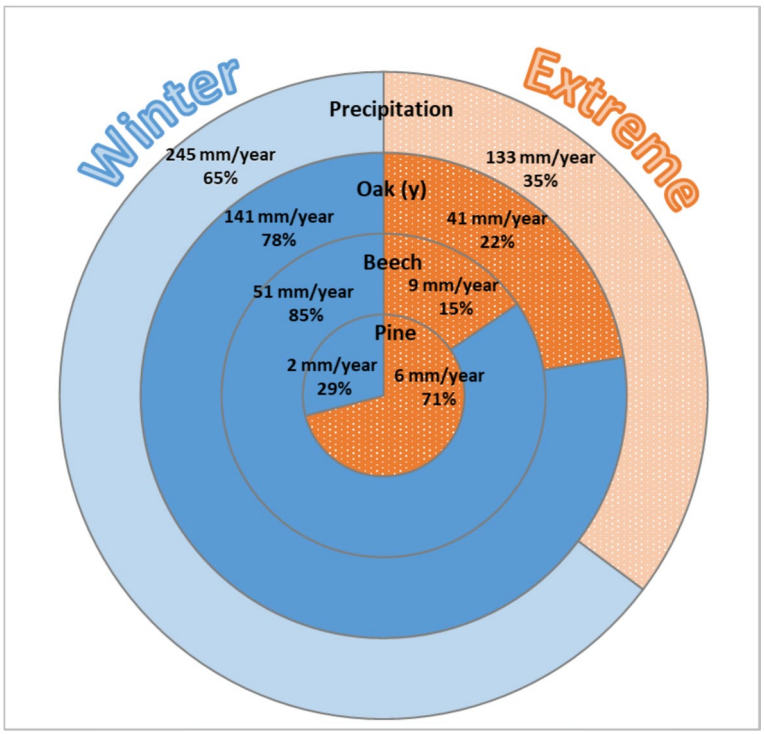

Fig. 5 Comparison between average winter-fed and extreme event-fed deep seepage as measured by lysimeters for the beech, oak(y), and pine stands and precipitation between 2018 and 2021

(pine) of deep seepage (Fig. 5), the intense precipitation events described by Sobaga et al. (2024) represented 15% of the annual precipitation and generated between 8% and 18% of the annual lysimeters' recharge.

Despite the unique opportunity of quantifying deep seepage with lysimeters, several limitations exist. An often-discussed issue of lysimeters is the boundary effects at the wall and on the bottom (e.g. Williams et al. 2020). Preferential fluxes might occur towards the wall of the lysimeter, which would result in an overestimation of deep seepage rates. However, in the large lysimeters used in the present study, the ratio between the perimeter (40 m) and surface area (100 m^2) was large and therefore minimised the influence of such effects on the estimated seepage rate. Wittenberg et al. (2019) reported a weak and delayed seepage response when a rainfall event occurred after a longer dry period. They assumed that in such cases, first, the adhesive pore water and the gravel layer at the bottom of the lysimeter were filled before drainage could begin, which implies an underestimation of Q_e if Q_w is finalised, which is what we observed during most events under pine and beech. Additionally, water overflow might be a source of inaccurate quantification of deep seepage. At IFMS Britz, the lysimeter collar protrudes approximately 5 cm above the soil surface. This has previously prevented overflow occurrence during heavy precipitation. In addition, the saturated water conductivity of the sand is very high with more than 2 m per day (A. G. Boden et al. 2024) compared with the mean precipitation intensities of 150 mm during 24 h (Event21) or 82 mm during 9 h (Event2020). We therefore conclude that those interferences are of lower magnitude (even negligible). This harmonises with no or negligible surface runoff in small inland forested subcatchments with high infiltration capacities of the northeastern German lowlands, without hydraulic connection to surface water or less slope (Wolters et al. 2023). Snow and frozen soil may influence the timing and portioning of water flows in the winter half-year. At the IFMS Britz, snow and frozen soil are not the focus of the measurements. As we have no surface runoff in the lysimeters, there could only be a temporal shift in soil rewetting and deep seepage, not influencing extreme summer precipitation events. Therefore, snow and frozen soil are neglected in this analysis. An impact of snow and frozen soil is unlikely, as there is an increasing available water content during winter (Fig. 4).

4.3 Water balance components of different stands

As shown above, most of the annual precipitation is returned to the atmosphere by evapotranspiration. The differences between the lysimeters under beech and under pine are consistent with the findings of previous studies at IFSM Britz (Müller and Bolte 2009). In pine stands, it takes longer to replenish the plant-available soil water before deep seepage can take place under a given precipitation regime. Young oak stands, like other younger forest stands, take up less water than older forest stands do (e.g., Mitscherlich 1981; Brown et al. 2005; Natkhin et al. 2012; Oishi, 2020). Leuschner et al. (2022) reported that high evapotranspiration in pine stands leads to little or no deep seepage; our setup confirms this reduced seepage under pine (Table 6). IFSM Britz was established to analyse the impact of different forest stands on the water balance under even boundary conditions (Lützke & Simon 1971). Therefore, a flat area with horizontal and vertical homogeneous sandy soils was chosen. As no replications were available and only four events were analysed, we are unable to generalise our observations to stand or species levels. Nevertheless, careful consideration of the general productivity of tree species depending on soil (Bončina et al. 2023) and climate conditions (Aitken et al. 2008) leads to changes in the water balance, limiting the transferability. Despite this limitation, the transferability seems high; the sandy beech, oak, and pine stands on the IFSM Britz are typical in terms of soil composition, climate, and topography to large stretches of the northeastern German lowlands. Müller (2019) characterises IFSM Britz as typical for two-thirds of forest stands in Brandenburg.

During extreme summer precipitation events, the relative impact of interception decreased, as the interception by the canopy is limited (Fernández and Trejo 2020; Junjun Yang et al. 2023). In addition, transpiration is usually low during such events, as vapour pressure deficit and solar radiation are low. The main difference between beech, oak (y), and pine stands can be found in the pre-event soil moisture (Table 5). The reasons for this are a lower leaf area index than that of beech stands, resulting in lower interception and transpiration (Table 2), and a less developed rooting depth of young trees. Differences in water balance between the analysed lysimeters also resulted from differences in the architecture of the trees. In contrast to pine, beech has a funnel-shaped crown—steeply sloping branches and twigs funnel water towards the stem—and smooth bark. This morphological peculiarity of beech means that during heavy rainfall events, a large amount of intercepted precipitation flows down the trunk of beech trees. Stemflow formation in beech stands concentrates and channels water in a circular pattern at the base of the trunk. From there, it flows preferentially along the roots into the subsoil (Schwärzel et al. 2012; Friesen 2020). Additionally, the absolute values of Q_e were highest under oak (y) and lowest for pine. However, Q_e under pine far exceeded Q_w.

5 Conclusion

Our lysimeter-based monitoring revealed high impacts of extreme summer precipitation events on deep seepage. During 2018 and 2021, about 71% (pine), 22% (young oak), and 22% (beech) of the annual deep seepage was contributed by extreme summer precipitation events. The observed increase in the frequency of extreme summer precipitation events and also the projected increase caused by changing climate patterns show the importance for deep seepage formation and have not been the focus thus far.

As the return period of such events has decreased, we conclude that for the dominating pine forests, rapid deep seepage formation during extreme summer precipitation may be the most important mechanism for recharging aquifers in the northeastern German lowlands in the future. The observed variations in deep seepage formation between the oak and beech stands are mainly due to differences in forest age.

However, the monitoring site setup indicates that silviculture in the form of tree species composition has the potential to compensate for some ecosystem service losses. Provided that these events will occur reliably in the future, forest management systems can play a substantial role in increasing groundwater recharge and mitigating groundwater scarcity-related conflicts.

Acknowledgements

We are very much aware that the findings that allowed this evaluation are a result of years of scientific observation performed by – meanwhile – generations of scientists and technicians at IFMS Britz, Germany. Therefore, our appreciation and special thanks go to Jürgen Müller, Claudia Sauer, Bernd Windschügl, Andreas Bahr, Björn Christen, and many more.

Authors' contributions

MN: conceptualization, methodology, investigation, data curation/ analysis, resources, writing – original draft. MS: conceptualization, methodology, writing – original draft, visualization. TGMS: supervision, writing – review & editing. TS: conceptualization, data curation / analysis, writing – original draft, visualization. KS: conceptualization, writing – original draft.

Funding

Open Access funding enabled and organized by Projekt DEAL. The research described in this manuscript was not supported by external funding.

Data availability

The data used in this manuscript is accessible at Natkhin M, Bahr A, Christen B, Strer M (2025) Data used for analysis of extreme precipitation events and their Impact on summer deep seepage on the Intensive Forest Monitoring Station Britz 2025. https://doi.org/10.3220/253-2025-175

Declarations

Competing interests

The authors declare no competing interests.

Author details
[1] Institute of Forest Ecosystems, Johann Heinrich von Thünen-Institute, Eberswalde, Germany.

Received: 14 July 2025 Accepted: 1 December 2025
Published online: 20 January 2026

References

Aitken SN, Yeaman S, Holliday JA, Wang T, Curtis-McLane S (2008) Adaptation, migration or extirpation: climate change outcomes for tree populations. Evol Appl 1:95–111. https://doi.org/10.1111/j.1752-4571.2007.00013.x

Beck HE, Zimmermann NE, McVicar TR, Vergopolan N, Berg A, Wood EF (2018) Present and future Köppen-Geiger climate classification maps at 1-km resolution. Sci Data 5:180214. https://doi.org/10.1038/sdata.2018.214

Boden AG, Finnern H, Grottenthaler W, Kühn D, Pälchen W, Schraps W-G, Spon-agel H (1994) German Soil Survey Guidelines: 4th revised and extended edition, KA4. Schweizerbart Science Publishers, Stuttgart, Germany

Boden AG, Hartmann KJ, Bauriegel A, Dehner U, Eberhardt E, Hesse S, Kühn D, Martin W, Waldmann F (eds) (2024) German Soil Survey Guidelines: 6th completely revised and extended edition, KA6. Schweizerbart Science Publishers, Stuttgart, Germany

Boergens E, Güntner A, Dobslaw H, Dahle C (2020) Quantifying the Central European droughts in 2018 and 2019 with GRACE Follow-On. Geophys Res Lett 47:e2020GL087285. https://doi.org/10.1029/2020GL087285

Bončina A, Klopčič M, Trifković V, Ficko A, Simončič P (2023) Tree and stand growth differ among soil classes in semi-natural forests in Central Europe. CATENA 222:106854. https://doi.org/10.1016/j.catena.2022.106854

Brown AE, Zhang L, McMahon TA, Western AW, Vertessy RA (2005) A review of paired catchment studies for determining changes in water yield resulting from alterations in vegetation. J Hydrol 310:28–61. https://doi.org/10.1016/j.jhydrol.2004.12.010

Cools N, De Vos B. (2020) Part X: sampling and analysis of soil. Version 2020–1. UNECE ICP Forests Programme Co-ordinating Centre (ed.): Manual on methods and criteria for harmonized sampling, assessment, monitoring and analysis of the effects of air pollution on forests. Thünen Institute of Forest Ecosystems, Eberswalde, Germany, 29 p + Annex, ISBN: 978-3-86576-162-0. https://www.icp-forests.net/monitoring-and-research/icp-forests-manual

Courty LG, Wilby RL, Hillier JK, Slater LJ (2019) Intensity-duration-frequency curves at the global scale. Environ Res Lett 14:84045. https://doi.org/10.1088/1748-9326/ab370a

DIN 4049 (1992) Hydrology; basic terms. DIN, Berlin (Beuth) [Publ.: Deutsches Institut für Normung]. https://doi.org/10.31030/2525591

Djebou S, Dagbegnon C, Singh VP (2016) Impact of climate change on precipitation patterns: a comparative approach. Int J Climatol 36:3588–3606. https://doi.org/10.1002/joc.4578

Don A, Hagen C, Grüneberg E, Vos C (2019) Simulated wild boar bioturbation increases the stability of forest soil carbon. Biogeosciences 16:4145–4155. https://doi.org/10.5194/bg-16-4145-2019

Eckhardt K (2008) A comparison of baseflow indices, which were calculated with seven different baseflow separation methods. J Hydrol 352:168–173. https://doi.org/10.1016/j.jhydrol.2008.01.005

Fernández T, Trejo I (2020) Rainfall interception based on indirect methods: a case study in temperate forests in Oaxaca, Mexico. JAWRA J Am Water Resour Assoc 56:712–723. https://doi.org/10.1111/1752-1688.12844

Fischer EM, Knutti R (2015) Anthropogenic contribution to global occurrence of heavy-precipitation and high-temperature extremes. Nat Clim Chang 5:560–564. https://doi.org/10.1038/nclimate2617

Friesen J (2020) Flow pathways of throughfall and stemflow through the subsurface. In: Van Stan, II, John T, Gutmann E, Friesen J (eds) Precipitation Partitioning by Vegetation: A Global Synthesis. Springer International Publishing, Cham, pp 215–228. https://doi.org/10.1007/978-3-030-29702-2_13

Gong C, Zhang Z, Wang W, Duan L, Wang Z (2021) An assessment of different methods to determine specific yield for estimating groundwater recharge using lysimeters. Sci Total Environ 788:147799. https://doi.org/10.1016/j.scitotenv.2021.147799

Hänsel S, Hoy A, Brendel C, Maugeri M (2022) Record summers in Europe: variations in drought and heavy precipitation during 1901–2018. Int J Climatol 42:6235–6257. https://doi.org/10.1002/joc.7587

Haydon SR, Benyon RG, Lewis R (1997) Variation in sapwood area and throughfall with forest age in mountain ash (*Eucalyptus regnans* F. Muell.). J Hydrol 187:351–366. https://doi.org/10.1016/S0022-1694(96)03016-8

Hosseinzadehtalaei P, Tabari H, Willems P (2020) Climate change impact on short-duration extreme precipitation and intensity–duration–frequency curves over Europe. J Hydrol 590:125249. https://doi.org/10.1016/j.jhydrol.2020.125249

Ibebuchi CC (2022) Patterns of atmospheric circulation in Western Europe linked to heavy rainfall in Germany: preliminary analysis into the 2021 heavy rainfall episode. Theor Appl Climatol 148:269–283. https://doi.org/10.1007/s00704-022-03945-5

Ionita M, Nagavciuc V (2021) Changes in drought features at the European level over the last 120 years. Nat Hazards Earth Syst Sci 21:1685–1701. https://doi.org/10.5194/nhess-21-1685-2021

IUSS Working Group WRB (2022) World Reference Base for Soil Resources. International soil classification system for naming soils and creating legends for soil maps, 4th edn., Vienna, Austria, ISBN 979-8-9862451-1-9. https://files.isric.org/public/documents/WRB_fourth_edition_2022-12-18.pdf

Kaiser K, Koch PJ, Mauersberger R, Stüve P, Dreibrodt J, Bens O (2014) Detection and attribution of lake-level dynamics in north-eastern Central Europe in recent decades. Reg Environ Change 14:1587–1600. https://doi.org/10.1007/s10113-014-0600-5

Kissel M, Schmalz B (2020) Comparison of baseflow separation methods in the German Low Mountain Range. Water. https://doi.org/10.3390/w12061740

Kottek M, Grieser J, Beck C, Rudolf B, Rubel F (2006) World Map of the Köppen-Geiger climate classification updated. Meteorologische Zeitschrift 15:259–263. https://doi.org/10.1127/0941-2948/2006/0130

Krause S, Sanders TG, Mund J-P, Greve K (2019) Uav-based photogrammetric tree height measurement for intensive forest monitoring. Remote Sens. https://doi.org/10.3390/rs11070758

Kreienkamp F, Philip SY, Tradowsky JS, Kew SF, Lorenz P, Arrighi J, Belleflamme A et al (2021) Rapid attribution of heavy rainfall events leading to the severe flooding in Western Europe during July 2021. FZJ-2022-00916 Report, World Weather Attribution 51 p. http://hdl.handle.net/2128/30381

Lazoglou G, Anagnostopoulou C, Tolika K, Kolyva-Machera F (2019) A review of statistical methods to analyze extreme precipitation and temperature events in the Mediterranean region. Theor Appl Climatol 136:99–117. https://doi.org/10.1007/s00704-018-2467-8

Leilei X, Jinglin L, Changjie J, Anzhi W, Dexin G, Jiabing W, Fenghui Y (2011) Baseflow separation methods in hydrological process research: a review. Chin J Appl Ecol 22(11):3073-3080 [in Chinese]

Leuschner C, Förster A, Diers M, Culmsee H (2022) Are northern German Scots pine plantations climate smart? The impact of large-scale conifer planting on climate, soil and the water cycle. For Ecol Manage 507:120013. https://doi.org/10.1016/j.foreco.2022.120013

Lischeid G, Dannowski R, Kaiser K, Nützmann G, Steidl J, Stüve P (2021) Inconsistent hydrological trends do not necessarily imply spatially heterogeneous drivers. J Hydrol 596:126096. https://doi.org/10.1016/j.jhydrol.2021.126096

Ludwig P, Ehmele F, Franca MJ, Mohr S, Caldas-Alvarez A, Daniell JE, Ehret U, Feldmann H, Hundhausen M, Knippertz P, Küpfer K, Kunz M, Mühr B, Pinto JG, Quinting J, Schäfer AM, Seidel F, Wisotzky C (2023) A multi-disciplinary analysis of the exceptional flood event of July 2021 in Central Europe - Part 2: Historical context and relation to climate change. Nat Hazards Earth Syst Sci 23:1287–1311. https://doi.org/10.5194/nhess-23-1287-2023

Lützke R, Simon KH (1971) Untersuchungen zum Wasserhaushalt und Wasserverbrauch der Kiefer auf pleistozänen Sanden: FE-Bericht, Institut für Forstwissenschaften. Eberswalde, GDR. 71 p.

Meißner R, Prasad MNV, Du Laing G, Rinklebe J (2010) Lysimeter application for measuring the water and solute fluxes with high precision. Curr Sci 99:601–607

Metzger M, Bunce RG, Leemans R, Viner D (2008) Projected environmental shifts under climate change: European trends and regional impacts. Environ Conserv 35:64–75. https://doi.org/10.1017/S0376892908004529

Miegel K, Mehl D, Malitz G, Ertel H (2014) Ungewöhnliche Niederschlagsereignisse im Sommer 2011 in Mecklenburg-Vorpommern und ihre hydrologischen Folgen. Teil 1 (Unusual rainfall events in Mecklenburg-Vorpommern during the summer of 2011 and their hydrological consequences – Part 1: Hydrometeorological event appraisal). Hydrol Wasserbewirtsch 58:280–302

Mitscherlich G (1981) Wald, Wachstum und Umwelt - Eine Einführung in die ökologischen Grundlagen des Waldwachstums: 2. Band - Waldklima und Wasserhaushalt. J. D. Sauerländer's Verlag, Frankfurt am Main

Müller J (2019) Die Forsthydrologische Forschung im Nordostdeutschen Tiefland: Veranlassung, Methoden, Ergebnisse und Perspektiven. Schriftenreihe Umweltingenieurwesen, vol 91, Rostock, ISBN 978-3-86009-491-4, 358 p.

Müller J, Bolte A (2009) The use of lysimeters in forest hydrology research in North-East Germany. Landbauforsch VTI Agric for Res 59:1–10

Natkhin M, Steidl J, Dietrich O, Dannowski R, Lischeid G (2012) Differentiating between climate effects and forest growth dynamics effects on decreasing groundwater recharge in a lowland region in northeast Germany. J Hydrol 448:245–254. https://doi.org/10.1016/j.jhydrol.2012.05.005

Natkhin M, Bahr A, Christen B, Strer M (2025) Data used for analysis of extreme precipitation events and their Impact on summer deep seepage on the Intensive Forest Monitoring Station Britz 2025. https://doi.org/10.3220/253-2025-175

Oishi AC, Denham SO, Brantley ST, Novick KA, Bolstad PV, Miniat CF (2020) Quantifying the effects of stand age on components of forest evapotranspiration. In: Acta Horticulturae. International Society for Horticultural Science (ISHS), Leuven, Belgium, pp 89–96. https://doi.org/10.17660/ActaHortic.2020.1300.12

Passow C, Donner RV (2019) A rigorous statistical assessment of recent trends in intensity of heavy precipitation over Germany. Front Environ Sci. https://doi.org/10.3389/fenvs.2019.00143

Pendergrass AG, Knutti R, Lehner F, Deser C, Sanderson BM (2017) Precipitation variability increases in a warmer climate. Sci Rep 7:17966. https://doi.org/10.1038/s41598-017-17966-y

Qing Y, Wang S, Yang Z-L, Gentine P (2023) Soil moisture–atmosphere feedbacks have triggered the shifts from drought to pluvial conditions since 1980. Communications Earth & Environment 4:254. https://doi.org/10.1038/s43247-023-00922-2

Rakovec O, Samaniego L, Hari V, Markonis Y, Moravec V, Thober S, Hanel M, Kumar R (2022) The 2018–2020 multi-year drought sets a new benchmark in Europe. Earths Future 10:e2021EF002394. https://doi.org/10.1029/2021EF002394

Raspe S, Fleck S, Beuker E, Preuhsler T, Bastrup-Birk A (2020) Manual on methods and criteria for harmonized sampling, assessment, monitoring and analysis of the effects of air pollution on forests: meteorological measurements. UNECE ICP Forests, Programme Co-ordinating Centre, Eberswalde, Germany. 18 p. + Annex. ISBN: 978-3-86576-162-0. https://www.icp-forests.net/monitoring-and-research/icp-forests-manual

R Core Team (2022) R: A Language and Environment for Statistical Computing. R Foundation for Statistical Computing, Vienna, Austria. https://www.rproject.org/

Richter D (1995) Ergebnisse methodischer Untersuchungen zur Korrektur des systematischen Meßfehlers des Hellmann-Niederschlagsmessers. Berichte des Deutschen Wetterdienstes, vol 194. Deutsche Wetterdienst, Offenbach am Main ISBN 3-88148-309-8, 93 p.

Sanders TG, Natkhin M (2025) DEIMS-SDR: Hydrological research site Britz - Germany. https://deims.org/8ee82a9b-5086-4547-b5aa-4064e3314762. Accessed 28 September 2025

Scanlon BR, Healy RW, Cook PG (2002) Choosing appropriate techniques for quantifying groundwater recharge. Hydrogeol J 10:18–39. https://doi.org/10.1007/s10040-001-0176-2

Schwaiger F, Poschenrieder W, Rötzer T, Biber P, Pretzsch H (2018) Groundwater recharge algorithm for forest management models. Ecol Modell 385:154–164. https://doi.org/10.1016/j.ecolmodel.2018.07.006

Schwärzel K, Menzer A, Clausnitzer F, Spank U, Häntzschel J, Grünwald T, Köstner B, Bernhofer C, Feger K-H (2009) Soil water content measurements deliver reliable estimates of water fluxes: a comparative study in a beech and a spruce stand in the Tharandt Forest (Saxony, Germany). Agric For Meteorol 149:1994–2006. https://doi.org/10.1016/j.agrformet.2009.07.006

Schwärzel K, Ebermann S, Schalling N (2012) Evidence of double-funneling effect of beech trees by visualization of flow pathways using dye tracer. J Hydrol 470:184–192. https://doi.org/10.1016/j.jhydrol.2012.08.048

Sobaga A, Habets F, Beaudoin N, Léonard J, Decharme B (2024) Decreasing trend of groundwater recharge with limited impact of intense precipitation: evidence from long-term lysimeter data. J Hydrol 637:131340. https://doi.org/10.1016/j.jhydrol.2024.131340

Tabari H (2020) Climate change impact on flood and extreme precipitation increases with water availability. Sci Rep 10:13768. https://doi.org/10.1038/s41598-020-70816-2

Vicente-Serrano SM, Lopez-Moreno J-I, BeguerLorenzo-Lacruz J, Sanchez-Lorenzo A, GarcAzorin-Molina C, Morán-Tejeda E, Revuelto J, Trigo R, Coelho F, Espejo F (2014) Evidence of increasing drought severity caused by temperature rise in southern Europe. Environ Res Lett 9:44001. https://doi.org/10.1088/1748-9326/9/4/044001

Deutscher Wetterdienst (2018) The Monthly Climate Status of Germany July 2018 (in German), Offenbach. https://www.dwd.de/klimastatus

Deutscher Wetterdienst (2019) The Monthly Climate Status of Germany June 2019 (in German), Offenbach. https://www.dwd.de/klimastatus

Deutscher Wetterdienst (2020) The Monthly Climate Status of Germany June 2020 (in German), Offenbach. https://www.dwd.de/klimastatus

Williams MR, Coronel O, McAfee SJ, Sanders LL (2020) Preferential flow of surface-applied solutes: effect of lysimeter design and initial soil water content. Vadose Zone J 19:e20052. https://doi.org/10.1002/vzj2.20052

Wittenberg H (1999) Baseflow recession and recharge as nonlinear storage processes. Hydrol Process 13:715–726

Wittenberg H, Sivapalan M (1999) Watershed groundwater balance estimation using streamflow recession analysis and baseflow separation. J Hydrol 219:20–33. https://doi.org/10.1016/S0022-1694(99)00040-2

Wittenberg H, Aksoy H, Miegel K (2019) Fast response of groundwater to heavy rainfall. J Hydrol 571:837–842. https://doi.org/10.1016/j.jhydrol.2019.02.037

Wolters T, McNamara I, Tetzlaff B, Wendland F (2023) Germany-wide high-resolution water balance modelling to characterise runoff components as input pathways for the analysis of nutrient fluxes. Water. https://doi.org/10.3390/w15193468

Wunsch A, Liesch T, Broda S (2022) Deep learning shows declining groundwater levels in Germany until 2100 due to climate change. Nat Commun 13:1221. https://doi.org/10.1038/s41467-022-28770-2

Yang J, He Z, Feng J, Lin P, Jun Du, Guo L, Liu Y, Yan J (2023) Rainfall interception measurements and modeling in a semiarid evergreen spruce (*Picea crassifolia*) forest. Agric for Meteorol 328:109257. https://doi.org/10.1016/j.agrformet.2022.109257

Publisher's Note